MAGNETIC PROPERTIES OF TETRATAENITE-RICH STONY METEORITES

Takesi NAGATA and Minoru FUNAKI

National Institute of Polar Research, 9–10, Kaga 1-chome, Itabashi-ku, Tokyo 173

Abstract: Three chondrites, Yamato-74160 (LL7), ALH-77260 (L3) and St. Séverin (LL6), contain considerable amount of the ordered FeNi, tetrataenite, in their metallic components. The thermomagnetic curves of these tetrataenite-rich chondrites are characterized by a very flat heating curve up to 400–450°C and then an abrupt decrease to Curie point which ranges between 550–580°C. NRM of these chondrites contains a highly stable component which can be hardly demagnetized by alternating magnetic fields up to 1800 Oe peak. The highly stable component is identified to NRM of the tetrataenite phase which has a large magnetic and optical anisotropy. By heating up to 800°C, however, the tetrataenite phase is broken down, by the order-disorder transformation, to the ordinary disordered taenite which has a much weaker magnetic coercivity.

1. Introduction

It was experimentally demonstrated by NÉEL *et al.* (1964) that an ordered crystal of 50% Fe–50% Ni in atomic ratio of tetragonal structure (AuCu type) can be formed by neutron irradiation of an ordinary disordered taenite crystal of the same chemical composition at 295°C in presence of a magnetic field (2.5 kOe) parallel to one of [100] axes of its fcc crystal structure. Since the unit cell of ordered state of FeNi is tetragonal, it has uniaxially anisotropic characteristics with the easy direction of magnetization along [100] axis, similarly in the case of a hexagonal cobalt crystal. The magnetic anisotropy energy (E) of an ordered FeNi crystal has been measured to be approximately presented by

$$E = K_1 \sin^2\theta + K_2 \sin^4\theta, \tag{1}$$

where θ denotes the angle between the magnetization and the [100] direction, and $K_1 = 3.2 \times 10^6$ ergs/cm^3 and $K_2 = 2.3 \times 10^6$ ergs/cm^3 (NÉEL *et al.*, 1964). The observed intensity of saturation magnetization (J_s) of ordered FeNi is about 1300 emu/cm^3, which is approximately same as that of disordered FeNi (taenite).

The ordinary disordered FeNi crystal of 50%Fe–50%Ni in chemical composition has a fcc crystal structure and its K_1 is about 5×10^3 ergs/cm^3 (*e.g.* HALL 1959). Therefore, the magnetic anisotropy energy of the ordered FeNi is extremely large in comparison with that of the ordinary disordered FeNi of the same chemical composition. The order-disorder transition temperature of a FeNi crystal is 320°C (NÉEL *et al.*, 1964).

The presence of the ordered FeNi metallic grains has been found and confirmed by use of various crystallographic analysis techniques in 2 chondrites and 2 mesosiderites

(GOOLEY *et al.*, 1975), in Toruca Ni-rich ataxite (ALBERTSEN *et al.*, 1978), in Santa Catharina Ni-rich ataxite (DANON *et al.*, 1979a), in St. Séverin LL6 chondrite and 7 other meteorites (DANON *et al.*, 1979b), in Estherville mesosiderite (METHA *et al.*, 1980). CLARKE and SCOTT (1980) have optically identified the presence of ordered FeNi grains in 61 meteorites (H, L and LL chondrites, mesosiderites, pallasites, irons and a diogenite) and have concluded that the so-called clear taenite often observed in meteorites is identical to the ordered FeNi phase which has a large optical anisotropy. Since the ordered FeNi metallic grains are naturally present in a large number of meteorites, a natural metallic mineral of 50% Fe–50% Ni in atomic ratio in chemical composition and in the ordered state of tetragonal structure of AuCu type has been named "tetrataenite" by CLARKE and SCOTT (1980).

In magnetic studies of meteorites, on the other hand, it has been noted that some meteorites, such as St. Séverin LL6 chondrite, have an unusually large magnetic coercive force (H_C) and have an unusually high stability of natural remanent magnetization (NRM) for the AF-demagnetization test (*e.g.* Nagata, 1979). As more than a half of metallic components in St. Séverin are tetrataenites (DANON *et al.*, 1979b), it seems most likely that its large value of H_C($H_C \simeq 500$ Oe) and high stability of NRM is due to the tetrataenite magnetization. Another example is the thermomagnetic curve of Santa Catharina Ni-rich ataxite which could not be reasonably well interpreted (LOVERING and PARRY, 1962) until it has been discovered (DANON *et al.*, 1979a) that Santa Catharina consists of tetrataenite phase of 50–51 wt% Ni and 48–49 wt% Fe and more heterogeneous ordinary taenite phase of 27 wt% Ni, where no kamacite nor plessite phase is detected and the bulk Ni-content is about 35 wt%. The tetrataenite phase in Santa Catharina was broken down to the ordinary taenite by keeping it at 460°C for about 10 hours (DANON *et al.*, 1979a). The breakdown of tetrataenite should be much faster at higher temperatures. Thus, the thermomagnetic curve of tetrataenite in Santa Catharina for the initial heating process up to higher temperatures above 600°C becomes unreproducible, the cooling thermomagnetic curve representing that of the transformed ordinary taenite.

In the present work, three stony meteorites which contain a considerably large amount of tetrataenite in their metallic component will be mineralogically and magnetically examined. The three stony meteorites are Yamato-74160 (LL7), ALH-77260 (L3) and St. Séverin (LL6) chondrites.

2. Yamato-74160 (LL7) Chondrite

Yamato-74160 is an extremely recrystallized LL chondrite (TAKEDA *et al.*, 1979) and is classified into LL7-group (TAKEDA and YANAI, 1980). According to TAKEDA *et al.* (1979), the representative composition of metallic component is given by (50.0% Fe, 46.7% Ni, 2.3% Co) in weight. It has been further suggested by these workers that the temperature of the last equilibration of this chondrite was 1090°C, which is considerably higher than 970°C for last equilibration temperature of ordinary chondrites.

2.1. Composition and structure of metals

Opaque minerals in Yamato-74160 observable under a reflection microscope are either FeNi metals or troilites (Fig. 1).

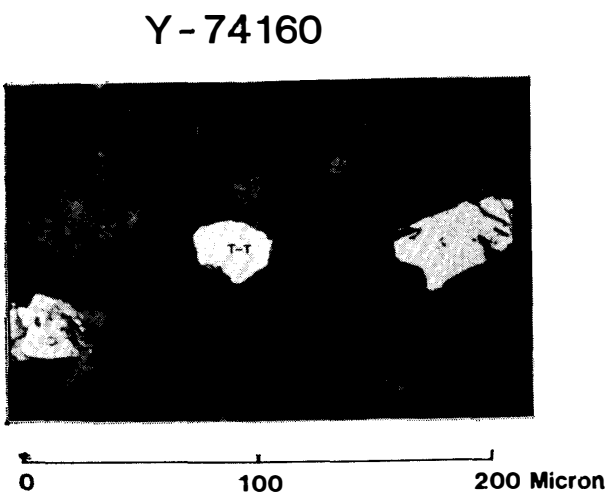

Fig. 1. Reflection microscope image of Yamato-74160.
T-T: Tetrataenite. Two other opaque minerals (white color in the photograph) are troilites.

The metallic FeNi grains are mostly 5–25 μm in their mean diameter and they are scattered isolatedly or connected to troilite of larger size in silicate matrix. Chemical compositions of 8 sites of 4 metallic grains measured by an electron-probe microanalyzer (EPMA) are summarized in Table 1, where ratio of Ni to Fe at each site is very close to 1 : 1 in atomic ratio. The average composition of observed metallic grains is given by (50.1% Fe, 47.9% Ni, 2.1%Co) in weight, which is in approximate agreement with the

Table 1. Chemical composition of metallic grains in Yamato-74160.

Grains	Site	Fe	Ni (wt%)	Co	Total (wt%)
A	A-1	49.06	48.13	2.10	99.29
B	B-1	51.35	48.23	2.24	101.82
	B-2	51.53	47.74	2.07	101.34
C	C-1	48.02	47.68	2.13	97.83
D	D-1	49.97	48.78	2.15	100.90
	D-2	49.52	46.97	2.29	98.78
	D-3	50.77	47.82	2.14	100.73
	D-4	50.26	47.91	1.97	100.14
Average		50.06	47.91	2.14	100.10

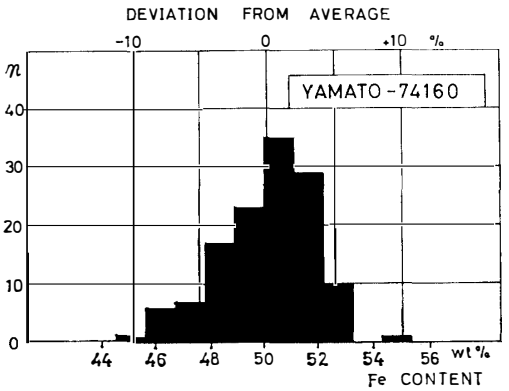

Fig. 2. Histogram of distribution of Fe-content within a surface of 140×115 μm of a tetrataenite grain in Yamato-74160.

result obtained by TAKEDA *et al.* (1979), and ratio of Fe-content to Ni-content in weight is very close to 1 to 1 in atomic ratio. The homogeneity of chemical composition within a polished surface of the largest one (D-grain) among four grains listed in Table 1 was examined with respect to the contents of Fe and Ni in further detail. Figure 2 shows a histogram of Fe-content measured by EPMA at 129 points of every 2 μm interval along mutually orthogonal X- and Y-axes (71 points along the major axis X and 58 points along the minor axis Y). As shown in Fig. 2, the most frequent value of Fe-content is about 50.5 wt% and the average value of Fe-content is about 50.1 wt%, while a half of the total measured spots are concentrated within a range of 49.0–51.3 wt% Fe, and Fe-contents at 84% of measuring points are gathered within a range of $\pm 5\%$ from the average value, namely within a range of 47.5–52.5 wt% Fe. This result indicates that the distribution of Fe-content over the surface of the clear taenite grain is homogeneous. A less quantitative EPMA analysis of Ni-content over the same surface shows that the distribution density of Ni also is homogeneous.

The optical anisotropy of the four metallic grains is examined under cross polars in a way as proposed by CLARKE and SCOTT (1980). The definitely detectable optical anisotropy of these metallic grains having about 50 wt% Fe are certainly identified to tetrataenites. No kamacite grain can be observed by the EPMA method in this chondrite. It is not certain, however, whether all metallic grains in this chondrite are tetrataenites or some of them are the ordinary taenites.

2.2. Basic magnetic properties

The magnetic hysteresis curves of Yamato-74160 are measured in a magnetic field range from -15 kOe to $+15$ kOe initially at 25°C and then at -269°C, and after heating up to 940°C, again at 25°C, -269°C and 21°C in sequence. Apparent saturation magnetization (I_s), saturated isothermal remanent magnetization (I_R), coercive force (H_C), remanence coercive force (H_{RC}) and apparent paramagnetic susceptibility (χ_p) measured at each temperature are summarized in Table 2. Remarkable results may be that both H_C and I_R after heating up to 940°C become much smaller than those before the heat treatment. $H_C=255$ Oe for the initial original state becomes $H_C=7$–8 Oe after heating up to 940°C, and $I_R=0.16$ emu/g for the original state becomes $I_R=(7\text{–}8)\times 10^{-3}$ emu/g after the heat treatment. It will be obvious that the marked decrease in H_C and I_R is due to a transformation of the magnetically coercive tetrataenite to the magnetically soft ordinary taenite by the heat treatment.

It should be noted, however, that the original value of $H_C=255$ Oe is still too small

Table 2. Magnetic hysteresis characteristics of Yamato-74160.

Magnetic parameter	Initial		After heating		
	25°C	−269°C	25°C	−269°C	21°C
I_s(emu/g)	1.59	1.80	2.36	3.45	2.50
I_R(emu/g)	0.16	0.24	8.0×10^{-3}	8.8×10^{-2}	6.5×10^{-3}
H_C(Oe)	255	226	8	51	7
H_{RC}(Oe)	460	775	240	3320	154
χ_p(emu/g/Oe)	7.5×10^{-5}	3.9×10^{-4}	2.9×10^{-5}	4.5×10^{-4}	3.7×10^{-5}

in comparison with a theoretically expected value of H_C for pure tetrataenite (about 5×10^3 Oe), though it is much larger than H_C of ordinary taenite (7–8 Oe). A most plausible interpretation of an apparent reduction of the H_C-value may be to attribute the reduction to an effect of a superposition of two ferromagnetic components, *i.e.* a component having a large value of H_C and the other one having a small value of H_C, as discussed for a case of lunar rocks (*e.g.* NAGATA *et al.*, 1972, 1974). In the present case of Yamato-74160, it seems most likely that some portion of 50% Fe–50% Ni metals are in the state of ordinary taenite while the remaining portion are tetrataenite in the initial original state. Using an analysis method described in a later section (Appendix A.1), and assuming that H_C=4900 Oe for tetrataenite and H_C=8 Oe for ordinary taenite, ratio of abundance of tetrataenite to that of oridinary taenite in the initial state is approximately estimated from measured data to be 0.40: 0.60.

I_s and χ_p before the heating in Table 2 may not be true saturation magnetization and paramagnetic susceptibility respectively, because tetrataenite component may not reach the saturation magnetization even in an external magnetic field of 15 kOe so that the measured value of magnetization at 15 kOe is smaller than the saturation magnetization, while χ_p-value estimated from the gradient of magnetization with respect to the external magnetic field in a high field range is larger than its true value. Actually, I_s before the heating is considerably smaller than I_s after the heating, while χ_p at room temperature before the heating is about twice the χ_p-value at the same temperature after the heating.

Another point noted in Table 2 may be considerable increases of I_R, H_C and H_{RC} at −269°C in comparison with those at room temperature after the heating procedure. The magnetic hysteresis curves of Yamato-74160 after heating up to 940°C were measured at −269, −240, −200, −150, −100 and 21°C. The observed values of I_R and H_C at respective temperatures are plotted in Fig. 3. It will be clear in Fig. 3 that both I_R and H_C become discontinuously larger at temperatures below a critical temperature between −200°C and −150°C. As already discussed for lunar rocks (NAGATA *et al.*, 1974), the observed sharp changes of I_R and H_C may be due to presence of very fine grains of single domain structure FeNi metal which are superparamagnetic at tempera-

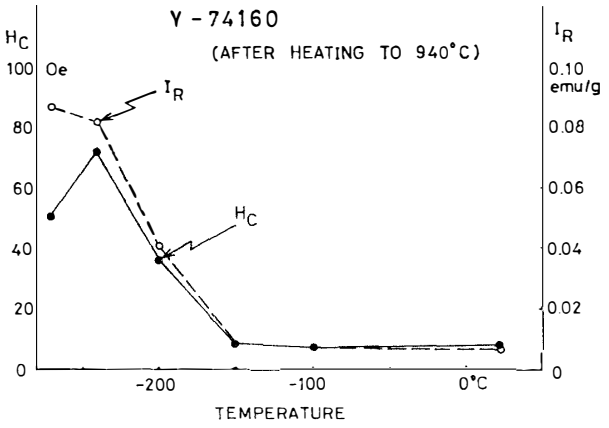

Fig. 3. Saturated IRM (I_R) and magnetic coercive force (H_C) of Yamato-74160 in a low temperature range below room temperature after heating to 940°C.

tures above a critical blocking temperature (T^*) but are ferromagnetic below T^*. The relaxation time (τ) of such superparamagnetic grains at temperature T is given by

$$\frac{1}{\tau}=f_0 \exp\left(-\frac{H_{RC}J_0 v}{2kT}\right),$$

where f_0 denotes an approximately constant coefficient of about $10^9 s^{-1}$ in magnitude, J_0 spontaneous magnetization of fine metallic grains per unit volume and v is average volume of the fine grains. τ is usually assumed to be 10^2 s at $T=T^*$. Since $J_0=1.3\times10^3$ emu/cm^3, $H_{RC}\simeq10^3$ Oe and $T^*\simeq100$ K, it can be concluded that $v\simeq5.4\times10^{-19}$ cm^3 or about 100 Å in mean diameter of individual metal particles. The presence of such fine metallic grains which are superparamagnetic at room temperature are detected in this chondrite after the heat treatment. A problem of whether the fine metallic grains are present in the original chondrite before the heating is difficult to be definitely solved, because magnetic effects of their presence are largely masked by the presence of magnetically coercive tetrataenite grains. Since $I_R(-269°C)$–$I_R(25°C)$ before the heating is approximately equal to $I_R(-269°C)$–$I_R(25°C)$ after the heating (Table 2), it could be assumed that these very fine metallic grains are present in the original unheated condition.

2.3. Thermomagnetic curve

Thermomagnetic curves of Yamato-74160 in a temperature range between −255°C and 800°C in a magnetic field of 10 kOe are shown in Fig. 4. The thermomagnetic measurements were carried out by a vibration magnetometer first by cooling from 25°C to −255°C, and then heating from −255°C to 800°C which gives the first-run heating thermomagnetic curve, and then cooling from 800°C to −255°C which gives the first-run cooling curve. The initial cooling thermomagnetic curve from 25°C to −255°C is practically identical to the first-run heating thermomagnetic curve from −255°C to 25°C.

In the first-run heating thermomagnetic curve, a sharp magnetic transition point at 560°C may correspond to Curie point of taenite of 56 wt% Ni, and a very small amount

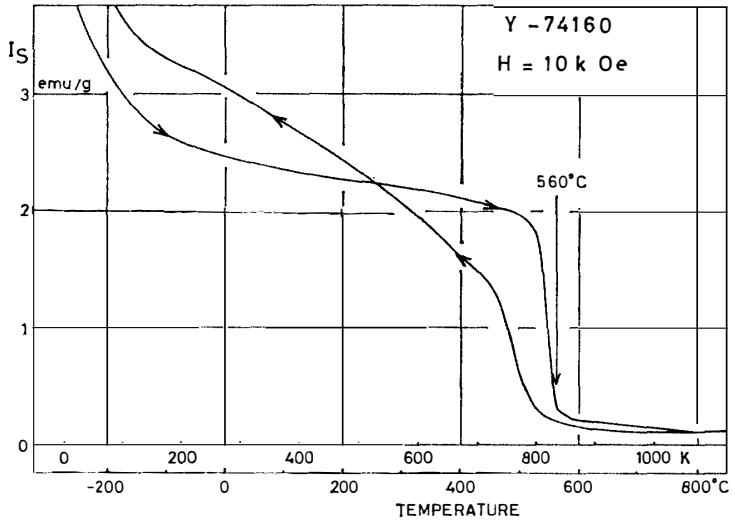

Fig. 4. First-run thermomagnetic curves of Yamato-74160.

of kamacite phase still remains up to about 780°C. At 800°C, the paramagnetic magnetization in 10 kOe is 0.074 emu/g, which indicates that the paramagnetic susceptibility at 25°C is 3.0×10^{-5} emu/g/Oe which is almost equal to the observed value of χ_p(25°C) after the heating.

In the first-run cooling thermomagnetic curve, the thermal change of magnetization below the magnetic transition at 560°C becomes much gentler than that in the first-run heating curve, and the magnetization intensity at room temperature after the heating becomes considerably larger than before the heating. The second-run heating and cooling thermomagnetic curves are almost identical to the first-run cooling curve. These measured results suggest that tetrataenite phase before the heating was almost completely transformed to ordinary taenite phase by heating up to 800°C in this experiment.

WASILEWSKI (1982) also has emphasized the difference between the heating and cooling thermomagnetic curves as a typical characteristic of tetrataenite in other tetrataenite-rich meteorites such as Estherville (mesosiderite) and Bjurbole (L4); namely, the shape of the tetrataenite thermomagnetic curve is essentially flat up to 500°C and then drops abruptly to Curie point, whereas the cooling curve is convex and resembles the thermomagnetic curve for ordinary ferromagnetic materials. The thermomagnetic characteristic is largely due to a difference of the magnetically unsaturated thermomagnetic curve of tetrataenite having an extremely large value of magnetic anisotropy in the heating curve from the magnetically saturated thermomagnetic curve of ordinary taenite having a small value of magnetic anisotropy in the cooling curve, as discussed in a later section (Appendix A.2).

2.4. *Natural remanent magnetization (NRM)*

The AF-demagnetization curves of natural remanent magnetization (NRM) of Yamato-74160 are shown in Fig. 5, where the right diagram shows the AF-demagnetization curve of NRM intensity while the left diagram illustrates changes of the direction of residual NRM during the course of AF-demagnetization up to 1800 Oe peak. By the AF-demagnetization up to 600 Oe peak, the NRM intensity considerably decreases and the NRM direction changes by about 30° in angle, but both the intensity and direction

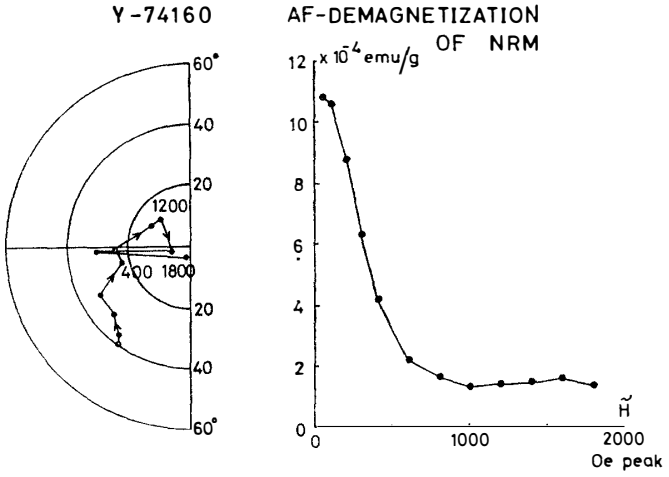

Fig. 5. AF-demagnetization curves of NRM of Yamato-74160. Left: Direction. Numerical figures indicate $\tilde{H}$-values. Right: Intensity.

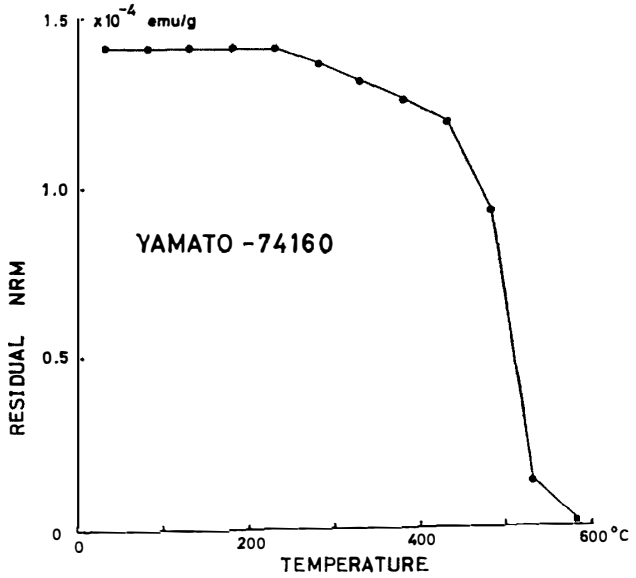

Fig. 6. Thermal demagnetization curve of the hard NRM-component of Yamato-74160, which remains after AF-demagnetizing up to 1800 Oe peak.

are kept almost constant for further AF-demagnetizations from 600 to 1800 Oe peak.

The thermal demagnetization curve of the residual NRM after the AF-demagnetization is shown in Fig. 6, where the direction of residual NRM during the course of thermal demagnetization up to 580°C is kept within a deviation circle of 6° in radius. It may be certain that the residual NRM after AF-demagnetizing to 1800 Oe peak is a very stable NRM component (larger than 1800 Oe in terms of microscopic magnetic coercivity) possessed by tetrataenite phase which has Curie point at about 560°C.

Simultaneously with the thermal demagnetization experiment, the Königisberger-Thellier experiments to produce the partial thermoremanent magnetization (PTRM) were carried out for each temperature, results being shown in Fig. 7. Although a plot for 480°C is considerably deviated from an approximate linear relation between PTRM acquired in a temperature range from T to 25°C and in a magnetic field of 0.50 Oe (abscissa) and residual NRM after thermal demagnetizing up to T (ordinate), it may be roughly concluded from Fig. 7 that a linear relationship approximately holds between the PTRM values and the residual NRM after the thermal demagnetization. If the magnetically hard component of NRM of Yamato-74160 remaining after the AF-demagnetization up to 1800 Oe peak is assumed to be attributable to TRM demonstrated by the present experiment, the paleointensity for the hard components of NRM is estimated to be 0.054 Oe. As already mentioned, however, considerable parts of tetrataenite phase should have been transformed to ordinary taenite by the stepwise heating procedures, the experimentally acquired PTRM may not present the true PTRM of tetrataenite phase which might have been acquired for a very long time in nature. It must be noted further that the ordinate values in Fig. 7 present only the residual hard component of NRM which has remained after AF-demagnetizing to 1800 Oe peak, whereas all ferromagnetic metals (including those whose NRM has been AF-demagnetized) are involved in the acquisition of PTRM on abscissa. Hence, the paleointensity for the hard magnetic component of Yamato-74160 may probably be much

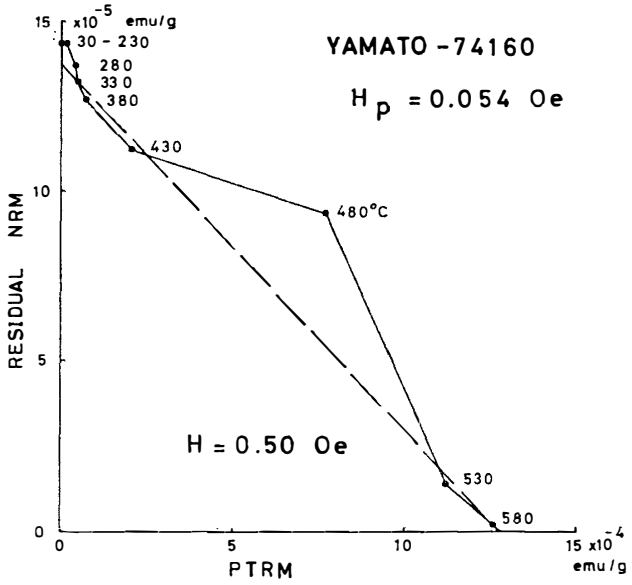

Fig. 7. Königisberger-Thellier plot for the hard NRM component of Yamato-74160 on a diagram of residual NRM after thermal demagnetization up to T vs. PTRM acquired by cooling from T in h=0.50 Oe.

larger than 0.054 Oe. Then, Figs. 5, 6 and 7 may simply indicate that (a) NRM of Yamato-74160 consists of two main components; one is a relatively soft component which is almost completely AF-demagnetized by about 600 Oe peak and the other is a hard component which is constant even in alternating magnetic fields up to 1800 Oe peak; (b) the hard component is nearly constant by thermal demagnetization up to the order-disorder transition temperature of tetrataenite (320°C) and sharply decreases at temperatures above 430°C down to zero at Curie point (560°C); (c) the acquisition of TRM takes place mostly in a cooling temperature range from Curie point to 430°C.

2.5. *Anhysteretic remanent magnetization (ARM)*

In Fig. 5, the soft component NRM takes about 85% parts of the total NRM. It may be certain that the soft component NRM is possessed mostly by ordinary taenite of about 50% Ni in atomic ratio, because most metals in Yamato-74160 have the chemical composition as indicated by a single sharp Curie point at 560°C.

As tetrataenite phase can be broken down to ordinary taenite by heating to high temperatures above the order-disorder transition temperature for a sufficiently long time, there will be a possibility to examine magnetic properties of the soft component NRM by comparing characteristics of anhysteretic remanent magnetization (ARM) before a heat treatment at an appropriate high temperature with those of ARM after the heat treatment. Figure 8 shows acquisition curves of ARM and AF-demagnetization curves of the acquired ARM before and after heating up to 800°C for Yamato-74160, where a given stationary magnetic field is 0.44 Oe. The ARM acquisition curve before the heat treatment becomes almost saturated at about 1000 Oe peak in alternating magnetic field ($\tilde{H}$) and the AF-demagnetization curve of ARM does not return zero at $\tilde{H}$=1800 Oe peak but keeps approximate constant beyond 1000 Oe peak. The ARM acquisition curve after the heat treatment increases by about 15% beyond $\tilde{H}$= 1000 Oe peak from that before the heat treatment, and the AF-demagnetization curve

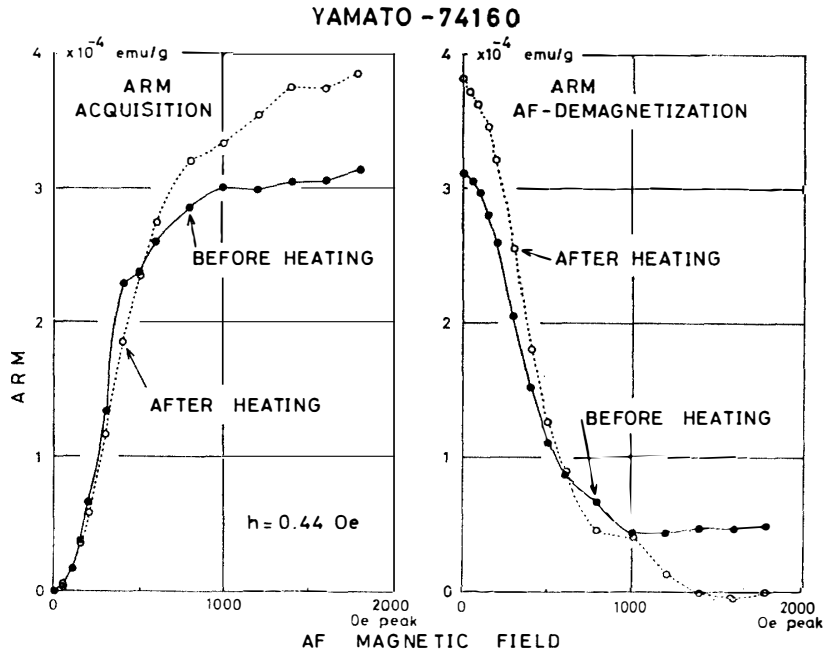

Fig. 8. ARM acquisition curves (left) and AF-demagnetization curves of ARM (right) of Yamato-74160 before and after heating to 800°C.

reaches approximate zero at $\tilde{H}$=1800 Oe peak.

These measured characteristics of ARM before and after the heat treatment seem to suggest the following points of metallic grains of Yamato-74160.

(a) The AF-demagnetization of ARM up to the maximum field for the ARM acquisition after the heat treatment has no residual, whereas that before the heat treatment has a residual of approximately constant magnitude in a higher field range of 1000–1800 Oe peak. This result seems to suggest that the initial state of zero magnetization of the ARM acquisition curve before heat treatment contains NRM of the hard component (*i.e.* tetrataenite) and the soft component domains which are so oriented that the total magnetization becomes zero. By the ARM acquisition process and AF-demagnetization of ARM, the soft component only reacts in response to the applied magnetic fields.

(b) Both ARM acquisition and AF-demagnetization of ARM are nearly completed in a field range of $\tilde{H}$=50–1000 Oe peak before the heating and the AF-demagnetization curve of ARM reasonably well resembles that of NRM shown in Fig. 4. Ratio of NRM-lost of ARM-lost for a field range of $\tilde{H}$=50–1000 Oe peak is given by ΔNRM/ΔARM=3.5, where ARM is acquired in a stationary magnetic field of 0.44 Oe. If the ratio (f_0) of acquisition rate of TRM to that of ARM in some weak magnetic field is known, the paleointensity (F_p) can be estimated by F_p=(0.44 Oe) ΔNRM/ΔARM/f_0 on an assumption that the NRM parts are acquired by the TRM acquisition mechanism. Even if f_0 assumes 10, F_p is evaluated to be about 0.15 Oe.

(c) ARM after the heating is larger by about 15% than ARM before the heating. The increase in ARM is most likely to be due to a result of a transformation of the magnetically hard tetrataenite phase to the magnetically soft ordinary taenite phase caused by the heat treatment.

3. ALH-77260 (L3) Chondrite

ALH-77260 is an L3 chondrite which contains small amounts of nickel-iron and troilite as opaque minerals (MASON, 1981).

3.1. Composition and structure of metals

Opaque minerals in ALH-77260 are kamacite, taenite and troilite. Results of EPMA measurements of chemical composition of 29 sites of 25 metallic grains in this L3 chondrite are shown in a Co-content versus Ni-content diagram in Fig. 9, where the remaining component is Fe. The metallic phases in ALH-77260 can be classified into 3 major groups, namely, a Co-rich kamacite group of 2.5–5.5 wt% Ni and about 1 wt% Co, a Co-poor kamacite group of 3.0–5.5 wt% Ni and about 0.5 wt% Co, and a taenite group of 35–52 wt% Ni and 0.1–0.3 wt% Co. A metallic grain of (72.18% Fe, 27.14% Ni, 0.68% Co) in composition may certainly be a mixture of the Co-rich kamacite phase and the taenite phase. For 4 relatively large metallic grains, their chemical compositions at 2 points for each grain are measured. They are (A) taenite grain of about

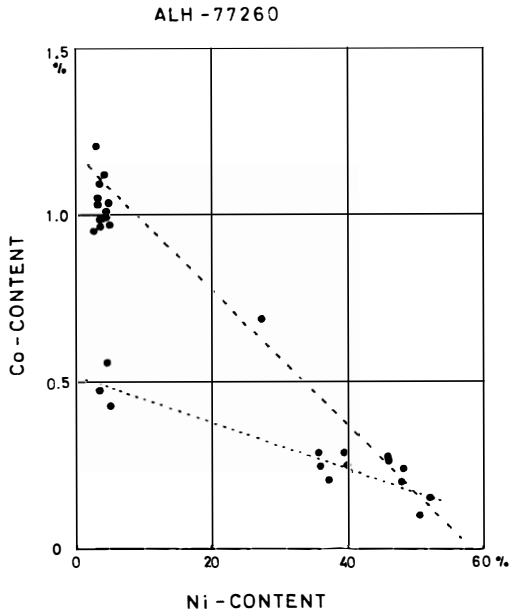

Fig. 9. Ni- and Co-contents in 25 metallic grains in ALH-77260 on a Co-content vs. Ni-content diagram. Remaining component is Fe.

170 μm in mean diameter and (60.56% Fe, 39.15% Ni, 0.29% Co in weight) and (63.69 % Fe, 36.06% Ni, 0.25% Co) in chemical composition, (B) a taenite grain of about 90 μm and (59.82% Fe, 39.93% Ni, 0.25% Co) and (51.58% Fe, 48.18% Ni, 0.24% Co), (C) a kamacite grain of about 80 μm and (94.65% Fe, 4.23% Ni, 1.12% Co) and (94.60% Fe, 4.41% Ni, 0.99% Co) and (D) a mixture of kamacite phase of (94.94% Fe, 4.08% Ni, 0.99% Co) and a taenite phase of (64.36% Fe, 35.35% Ni, 0.29% Co), where grain size is about 140 μm. All other measured metallic grains are 30–80 μm in their mean diameters. The homogeneity of chemical composition in individual metallic grains of about 10^2 μm in mean diameter can be observed in (A) and (B) taenite grains and (C) kamacite grain. Metallic grains consisting of kamacite and taenite phases such as (D) grain can be often observed in this chondrite. Figure 10 also shows an example of a metallic grain comprising kamacite and taenite. A metallic grain having

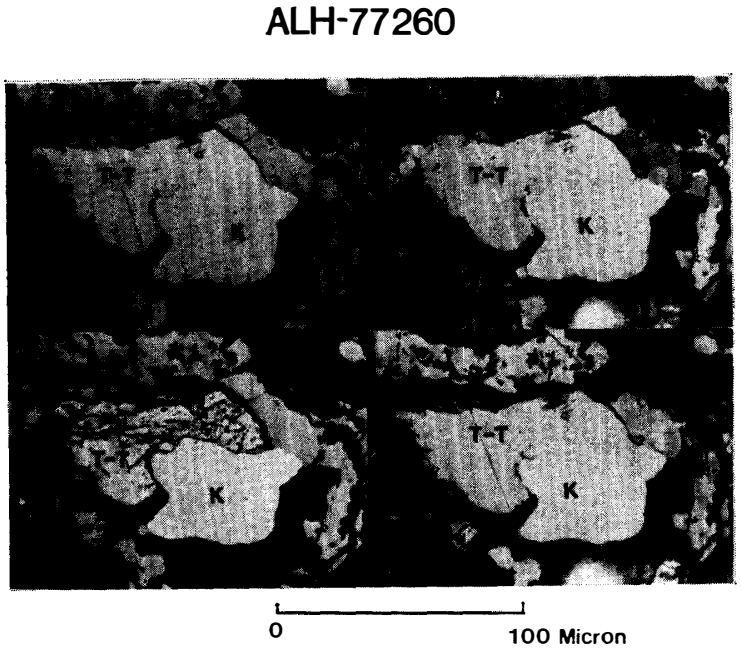

Fig. 10. Reflection microscope image of a metallic grain consisting of tetrataenite and kamacite phases in ALH-77260.
T-T: Tetrataenite, K: Kamacite.
Left top: Polished surface.
Right top: Under crossed polars (T-T and K are not distinguishable from each other).
Left bottom: Etched surface.
Right bottom: Under crossed polars (T-T can be distinguished from K).

an intermediate chemical composition (72.18% Fe, 27.14% Ni, 0.68% Co) shown at about the center of Co-Ni diagram in Fig. 9 is only 15 μm in mean diameter and attached to a larger troilite phase. Since its chemical composition is almost identical to a mixture of Co-rich kamacite phase and taenite phase in ratio 1: 1, this small metallic grain may comprise a half Co-rich kamacite and a half taenite.

The Co-content in the majority (14 grains) of kamacite ranges from 0.95 to 1.2 wt%, but that in 3 metallic grains is about 0.5 wt%. These 3 Co-poor kamacite grains are locally distributed within a distance range of about 0.25 mm. However, 14 grains of Co-rich kamacite and 11 grains of taenite are distributed apparently at random within an area of approximately 3.5×3.0 mm, no clearly defined texture for distribution of metallic grains of the different compositions being identified.

Relatively large grains of taenite of about 50 wt% Ni are the so-called clear taenites which show the characteristic optical anisotropy under nicols (*e.g.* CLARKE and SCOTT, 1980) as illustrated in Fig. 10. It is not much difficult to identify the tetrataenite phase which has the optical anisotropy in the case that tetrataenite phase is neighbored by other optically isotropic metallic phase as in case of Fig. 10, but it is not easy to optically identify isolated single phase grains of tetrataenite. It has been optically observed, however, that several large grains of taenite of about 50 wt% Fe in chemical composition are the clear taenites which can be identified to tetrataenites. Summarizing the results of EPMA measurements, it may be concluded that metallic components in ALH-77260 are kamacite of 3–5 wt% Ni, ordinary taenite of 35–45 wt% Ni, tetra-

Table 3. Magnetic hysteresis characteristics of ALH-77260.

Magnetic parameter	Specimen B				Specimen C			
	Before heating		After heating		Before heating		After heating	
	−269°C	30°C	30°C	−269°C	−269°C	30°C	30°C	−269°C
I_s (emu/g)	6.5	5.2	5.7	6.5	5.35	5.20	7.9	8.35
I_R (emu/g)	0.25	0.145	0.59	0.865	0.31	0.16	0.54	1.44
H_C (Oe)	86	83	180	240	81	86	120	270
H_{RC} (Oe)	1300	970	440	540	1450	1150	400	590
χ_p (emu/g/Oe)	5.5×10^{-4}	6.5×10^{-5}	3.5×10^{-5}	3.6×10^{-4}	3.25×10^{-4}	5.3×10^{-5}	2.0×10^{-5}	3.4×10^{-4}

taenite of about 50 wt% Ni and probably plessite of 25–30 wt% in average Ni-content.

3.2. Basic magnetic properties

The basic magnetic parameters of magnetic hysteresis phenomena (I_s, I_R, H_C, H_{RC} and χ_p) of 2 different pieces of ALH-77260 measured at 30°C and −269°C before heating up to 850°C in 10^{-5} Torr vacuum, and measured at 30°C and −269°C after the heating are summarized in Table 3.

In comparison with the magnetic hysteresis characteristics of Yamato-74160 (LL7) chondrite given in Table 2, those of ALH-77260 (L3) chondrite are fundamentally different; namely, both I_R and H_c considerably increase after the heating, though H_{RC} considerably decreases after the heating. Since the above-mentioned changes of the three magnetic parameters are qualitatively common in the two test specimens, these observed changes will be real and therefore need their reasonable interpretation.

As kamacite, ordinary taenite, tetrataenite and plessite coexist in the original condition of this chondrite, possible effects of homogenizing different metallic phases caused by the heating procedure should be much more complicated in comparison with the case of Yamato-74160. It seems likely, however, that a certain ferromagnetic phase which is largely magnetically coercive is newly produced by the heating of ALH-77260, because by the heating procedure the I_R value is increased to more than 3 times as large as its initial value before the heating in both specimens.

3.3. Thermomagnetic curves

Figures 11a and 11b show the first-run thermomagnetic curves of ALH-77260, specimens (B) and (C), for a temperature range between −269°C and 840°C. In the first-run heating curves, a sharp magnetic transition at 585°C for specimen (B) and at 570°C for specimen (C) may correspond to Curie points of taenite of 61 wt% Ni and that of 59 wt% Ni respectively, while the other magnetic transition at 780°C and at 775°C respectively may correspond to the $\alpha\rightarrow\gamma$ phase transition of kamacite. In the first-run cooling curve, the $\gamma\rightarrow\alpha$ transition begins to take place at about 700°C for specimen (B) and at about 690°C for specimen (C). These observed values of $\alpha\rightarrow\gamma$ and $\gamma\rightarrow\alpha$ transition temperatures indicate that the Ni-content in the kamacite phase is about 4 wt%. However, the slope of increase of I_s with decreasing temperature below the $\gamma\rightarrow\alpha$ transition temperature in the first-run cooling curves is very gradual, suggesting that Ni-content in kamacite after the heating is spread over a range of 4–7 wt% so that the $\gamma\rightarrow\alpha$ transition temperature also is spread over a range of 600–700°C, and further that

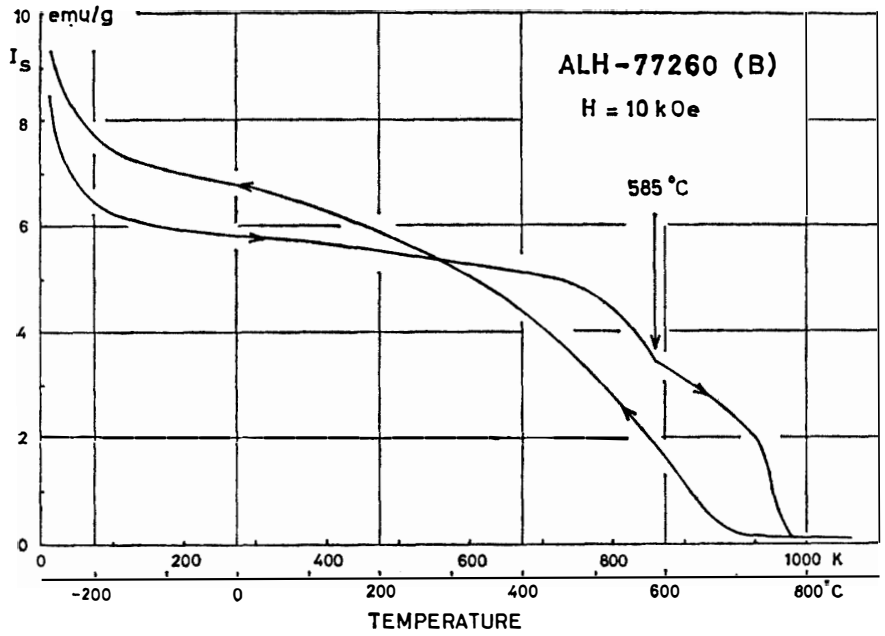

Fig. 11a. First-run thermomagnetic curves of ALH-77260. ALH-77260, specimen B.

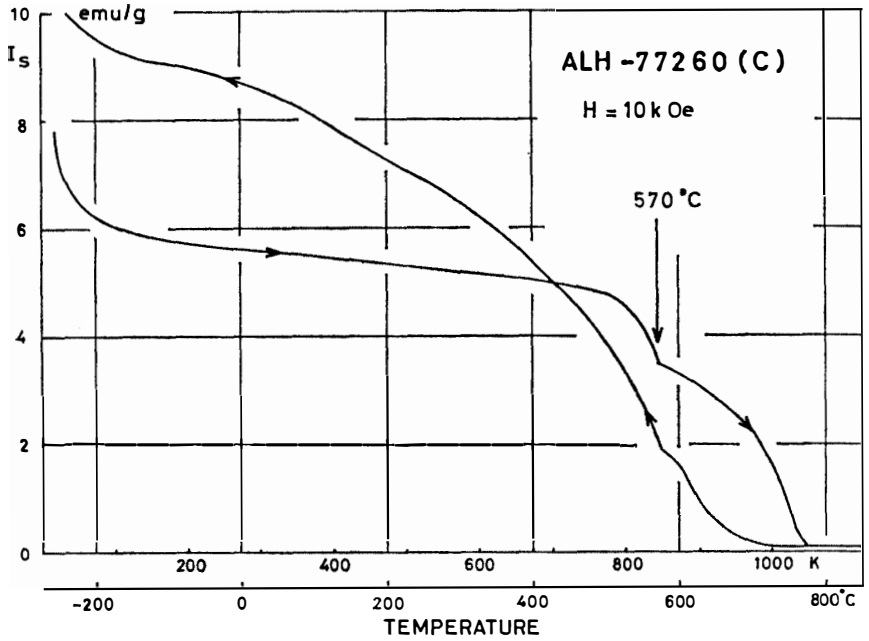

Fig. 11b. First-run thermomagnetic curves of ALH-77260. ALH-77260, specimen C.

Ni-content in taenite after the heating also is spread over a considerably large range, probably owing to a homogenizing with plessites and cloudy taenites by the heating.

Figures 12a and 12b show the second-run thermomagnetic curves in a temperature range between room temperature and 840°C, where magnetic transition temperature (Curie point) of taenite phase is 560–565°C, which correspond to about 56 wt% in Ni-content in taenite. $\alpha \rightarrow \gamma$ and $\gamma \rightarrow \alpha$ transition temperatures in the second-run thermomagnetic curves are $\Theta^*_{\alpha \rightarrow \gamma}$=785°C and 770°C and $\Theta^*_{\gamma \rightarrow \alpha}$=700°C and 695°C for speci-

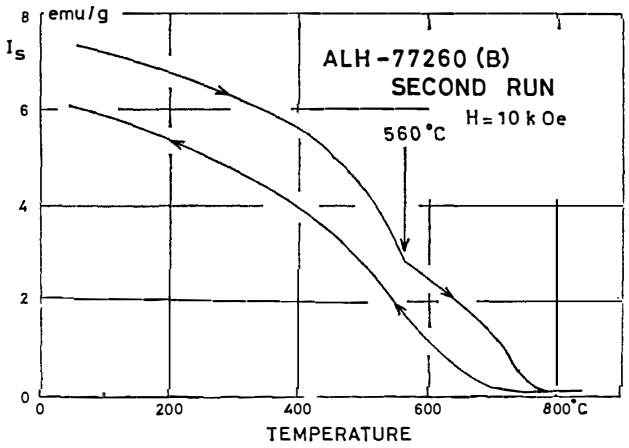

Fig. 12a. Second-run thermomagnetic curves of ALH-77260. ALH-77260, specimen B.

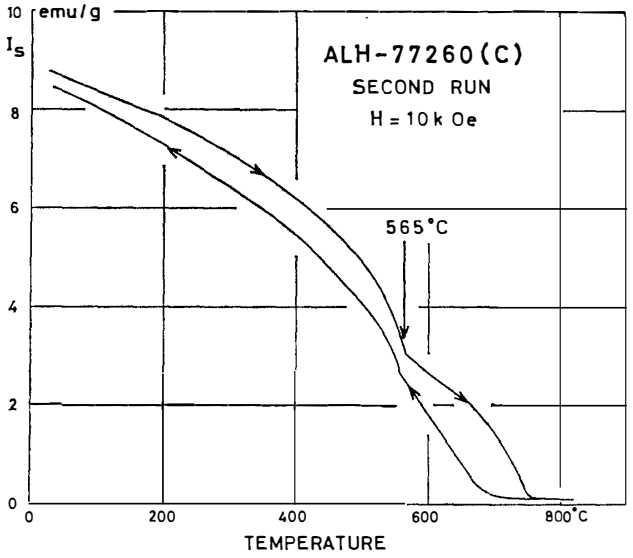

Fig. 12b. Second-run thermomagnetic curves of ALH-77260. ALH-77260, specimen C.

mens (B) and (C) respectively, suggesting that the lower limit of Ni-content in kamacite phase in the second heating process is almost same as that in the first heating process. It may be noticed in a comparison of Fig. 11 with Fig. 12, however, that the intensity of magnetization (I_s) of the kamacite phase in the second-run heating curve at temperatures above Curie point of taenite phase is considerably smaller than that in the first-run heating curve. The same difference in kamacite magnetization was observed in thermomagnetic curves of another specimen (ALH-77260 (A) obtained in preliminary test experiments, shown in Fig. 13). It may be concluded thus that the content of kamacite phase of 4–6 wt% Ni in metallic component of ALH-77260 is considerably reduced by heating to 840°C in 10^{-5} Torr atmosphere. Probably kamacite and taenite close to a boundary surface between them in metallic grains are homogenized by the heating procedure to produce taenite phase of less Ni-content. A little larger increasing rate of I_s with decreasing temperature even to about −100°C, illustrated in Figs. 11a and 11b, may indicate that Curie point of taenite phase after the heating procedure is distributed

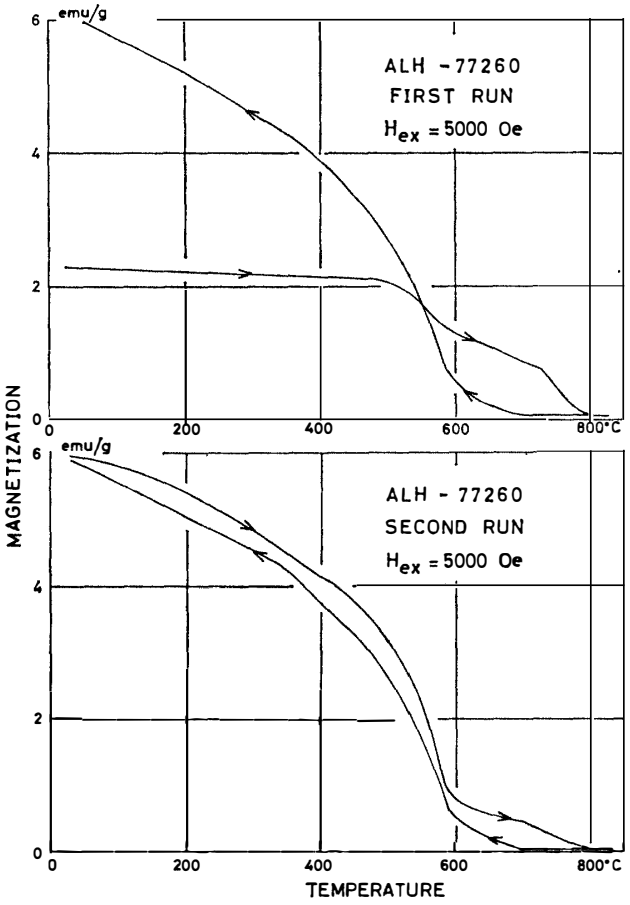

Fig. 13. First- and second-run thermomagnetic curves of ALH-77260, specimen A.

in a wide temperature range from 560°C to −100°C so that the Ni-content in individual taenite phases is distributed from 56 wt% down to less than 30 wt%. If the volume of the newly produced taenite phases are small enough to be of magnetic single domain structure, where the shape anisotropy is sufficiently large, the observed increase of H_C of ALH-77260 after the heating procedure could be reasonably interpreted. This plausible interpretation is, however, to be a possible presumption unless it can be experimentally confirmed.

A comparatively flat change and a relatively sharp decrease near 570–585°C of I_s with increasing temperature in the first-run heating thermomagnetic curves in Fig. 11 and Fig. 13 are largely due to the presence of tetrataenite phase which is transformed to the ordinary disordered taenite phase by the heating, just as in case of Yamato-74160 (see Appendix A.2).

3.4. Natural remanent magnetization

The AF-demagnetization curves of NRM intensity of three specimens (A), (B) and (C) of ALH-77260 are shown in Fig. 14. NRM of this chondrite also consists of a comparatively soft component which can be demagnetized by $\tilde{H}$=500–600 Oe peak and a harder component which can be hardly demagnetized even by $\tilde{H}$=1800 Oe peak. For the AF-demagnetization course of $\tilde{H}$=500–1800 Oe peak, the direction of residual

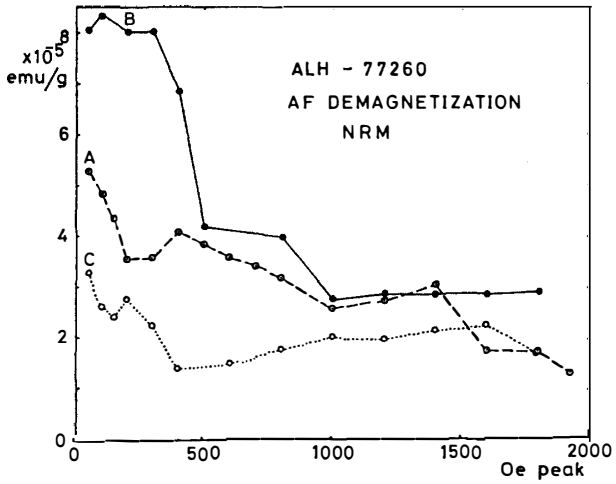

Fig. 14. AF-demagnetization curves of NRM intensity of ALH-77260, specimens A, B and C.

NRM is kept within a range of $\pm 15°$ in angle throughout the three cases. ALH-77260 chondrite contains, therefore, an extremely stable component of NRM which is practically kept constant for AF-demagnetization up to 1800 Oe peak.

A thermal demagnetization experiment on the residual NRM after AF-demagnetizing up to 1800 Oe peak was carried out on specimen (B) of ALH-77260. Although the residual NRM was systematically reduced by heating in 10^{-4} Torr atmosphere up to 270°C, (becoming about 56% of the initial value before the heating), the residual magnetization increased with fluctuations associated with vapor at temperatures above 320°C. It may thus be considered that the metallographic and chemical structures of ALH-77260, which is a considerably weathered L3 chondrite, are much more complicated in comparison with that of Yamato-74160. Hence, a paleomagnetic study of this chondrite will face much difficulty. With the Königisberger-Thellier technique for paleointensity studies, a reasonably good linear relation (within $\pm 5\%$ in error) holds between the residual NRM after a thermal demagnetization to temperature T and a PTRM acquired by cooling from T in presence of a weak magnetic field (h) for a temperature range between 20°C and 170°C, and an approximately linear relation (within $\pm 25\%$ in error) holds between them for a temperature range between 20°C and 270°C. For $h=0.50$ Oe, ΔNRM/ΔPTRM is 0.37 for temperature range of 20–170°C, and approximately 0.10 for 20–270°C. If we could ignore PTRM components acquired by kamacite and other metallic phases, paleointensity of the hard NRM component will be 0.185 or 0.05 Oe.

3.5. Anhysteretic remanent magnetization

In Fig. 14, NRM of ALH-77260 is classified into a hard component which appears to be due to tetrataenite and an additional soft component which can be mostly AF-demagnetized by 500–600 Oe peak of alternating magnetic field ($\tilde{H}$). Magnetic characteristics of the soft component may possibly be suggested by characteristics of ARM acquisition and AF-demagnetization of ARM insofar as applied alternating magnetic fields do not exceed a critical field to maintain the hard component invariant.

Figure 15 shows observed curves of acquisition of ARM and AF-demagnetization of the acquired ARM of specimens A, B and C of ALH-77260, where an applied

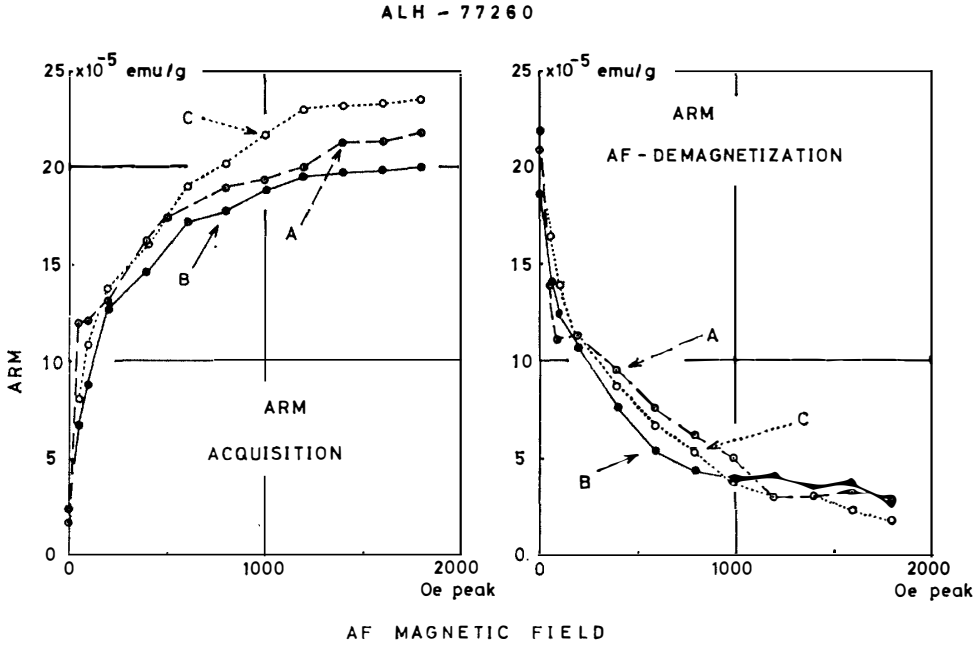

Fig. 15. ARM acquisition curves (left) and AF-demagnetization curves of ARM (right) of ALH-77260, specimens A, B and C. (Stationary magnetic field intensity (h) for ARM acquisition, h=0.48 Oe.)

stationary magnetic field (h) is 0.48 Oe. Although there are some quantitative discrepancies (about $\pm 10\%$) among the three specimens in both the ARM acquisition and the AF-demagnetization of ARM, it may be generally concluded that the ARM-acquisition is almost saturated by $\tilde{H}=1200$ Oe peak and the AF-demagnetization of ARM acquired by $\tilde{H}=1800$ Oe peak can be mostly completed by $\tilde{H}=1200$ Oe peak also. The initial values of magnetization at $\tilde{H}=0$ in the ARM acquisition curves and the final values of magnetization at $\tilde{H}=1800$ Oe peak in the AF-demagnetization curves present NRM of the hard component which is not affected by the experimental procedures by use of alternating magnetic fields smaller than 1800 Oe peak. Throughout the three observed curves, the distribution density of microscopic coercive force (h_c) is the largest in a range of $h_c=0$–100 Oe, and considerably large in a range of $h_c=100$–600 Oe, but it is almost zero for $h_c>1200$ Oe. The soft component whose microscopic coercive force is smaller than 1200 Oe may be identified to kamacite, plessite and ordinary taenite. Comparing the ARM acquisition curves and AF-demagnetization curves of ARM in Fig. 15 with the AF-demagnetization curves of NRM in Fig. 14, it may be noticed that the metallic components of $h_c<200$ Oe do not much contribute to NRM.

An approximate linear relationship holds between the AF-demagnetization curve of NRM and that of ARM for specimens A and B, which gives $F_p=\Delta\text{NRM}/\Delta\text{ARM}/f_0=0.39/f_0$ for specimen A and $F_p=0.84/f_0$ for specimen B. The soft component of NRM of specimen C is too small to be analyzed in the same way.

4. St. Séverin (LL6) Chondrite

As mentioned in the introduction of the present paper, St. Séverin (LL6) chondrite

contains a considerable amount of tetrataenite grains and its bulk magnetic coercive force amounts to 500 Oe.

4.1. Composition and structure of metals

The composition and structure of metallic grains in St. Séverin chondrite have been examined on the basis of Mössbauer spectra, scanning electron microscopy and X-ray measurements by DANON *et al.* (1979). The Mössbauer spectral analysis has shown that ratios of abundances of kamacite phase: tetrataenite phase: paramagnetic taenite phase in metals at room temperature are given by 39.9: 50.8: 9.5 in volume, and the chemical composition of ordered taenite (tetrataenite) phase is approximately given by 60%Fe 40%Ni.

Scanning electron micrographs have shown that the grain size of tetrataenite phase ranges from 0.15 to 0.30 μm, and weak superlattice structure lines of tetrataenite have been observed in the Debye-Scherrer diagram of X-ray diffraction photographs.

4.2. Basic magnetic properties

The observed magnetic hysteresis curve characteristics of a bulk sample of St. Séverin at room temperature are represented by $I_s=4.07$ emu/g, $I_R=0.54$ emu/g, $H_C=500$ Oe and $H_{RC}=1900$ Oe. In the present case, major ferromagnetic constituents in St. Séverin are kamacite and tetrataenite, where ordinary taenite phase (less than 30% Ni) is paramagnetic at room temperature. The observed value of H_C, 500 Oe, of this chondrite is the largest among H_C-values of a quite large number of the ordinary chondrites observed to date, which range from 3 to 160 Oe except for St. Séverin (LL6) and Yamato-74160 (LL6) (NAGATA, 1979). The high value of H_C of St. Séverin is very likely to be due to a high relative abundance of tetrataenite compared with that of kamacite in the ferromagnetic metallic component, as discussed in Appendix A.1.

4.3. Thermomagnetic curves

The thermomagnetic curves of magnetic grains of St. Séverin for the first- and second-run cycles are shown in Fig. 16. The measured sample is mostly composed of metallic phases, but is associated with some silicate minerals too.

The flat curve of magnetization up to about 400°C and its sharp decrease at about 550°C in the first-run heating curve will be a characteristic feature of a tetrataenite-rich chondrite, as observed in Yamato-74160 and ALH-77260 also. A magnetic transition in the first-run heating curve may correspond to Curie point of taenite of 56 wt% Ni. This result is in approximate agreement with the chemical composition of tetrataenite grains in St. Séverin measured by DANON *et al.* (1979). The first-run cooling thermomagnetic curve, below 550°C, however, is characterized by a concave form of continuous increase of magnetization with decreasing temperature, which represents a continuous spectrum of Ni-content extending between 30 and 56 wt% Ni in taenite.

As clearly shown in Fig. 16, the first-run heating thermomagnetic curve of St. Séverin consists of a kamacite phase of about 800°C in its $\alpha\rightarrow\gamma$ transition temperature ($\Theta^*_{\alpha\rightarrow\gamma}$) in addition to tetrataenite phase of 550°C in Curie point, while both the first-run and second-run cooling curves consist of a kamacite phase of 715°C in its $\gamma\rightarrow\alpha$ transition temperature ($\Theta^*_{\gamma\rightarrow\alpha}$) and taenite phase, whose Curie point is distributed in a wide temperature range from 550°C down to room temperature. Since the second-run heating curve is practically identical to the first-run and second-run cooling curves

for a temperature range from 20°C to 550°C, the taenite phase of continuously varying contents of Ni, produced by the first heating procedure, will be thermally stable.

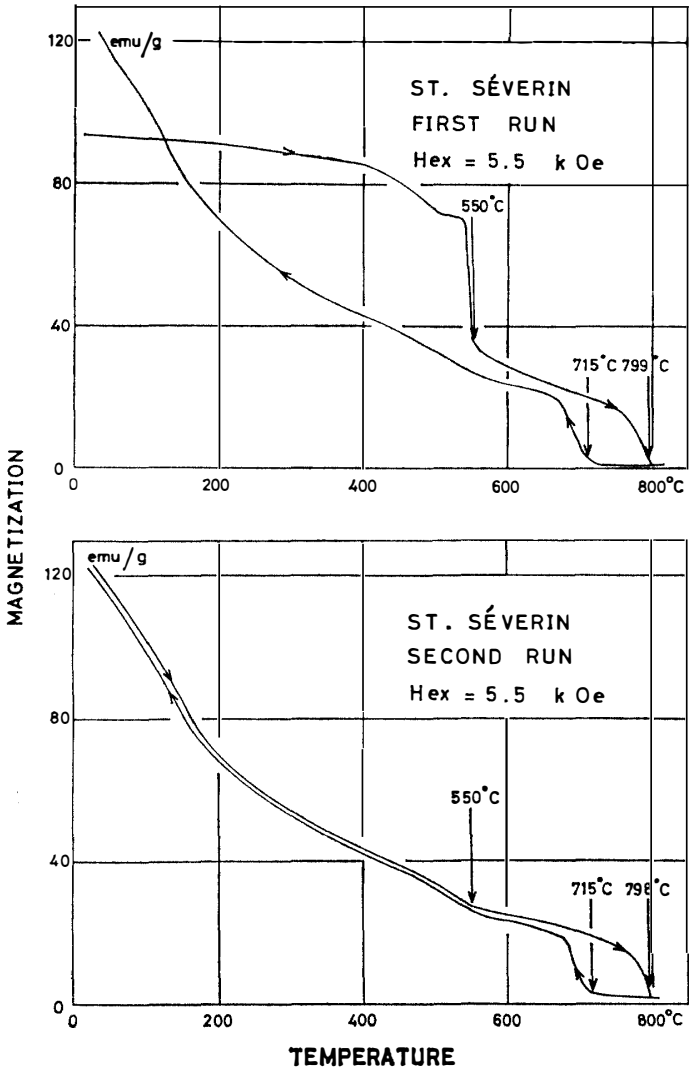

Fig. 16. First- and second-run thermomagnetic curves of St. Séverin.

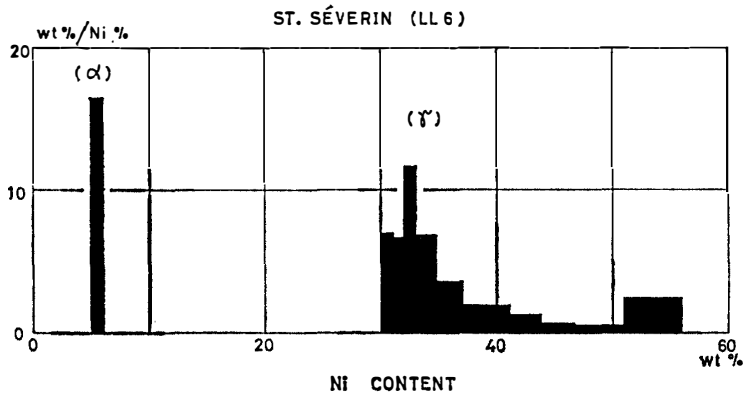

Fig. 17. Histogram of Ni-content in metallic component in St. Séverin after heating to 800°C in vacuum, obtained by a magnetic analysis.

The Ni-content of kamacite phase, in which $\Theta^*_{\alpha\to\gamma}=800°C$ and $\Theta^*_{\gamma\to\alpha}=715°C$, is estimated to be about 5 wt%. The Ni-content in taenite phase after the first heating procedure is obtained by a magnetic analysis of the first-run cooling curve on the basis of magnetic data of Fe-Ni alloys (CRANGLE and HALLAM, 1963). A histogram of Ni-content in kamacite and taenite phases after the heating procedure is given in Fig. 17, where the kamacite phase and the taenite phase occupy 16.4 and 72.2 wt% respectively of the examined sample. The observed conspicuous change from the first-run heating curve to the second-run heating curve for the taenite phase may be almost certainly due to a homogenization of tetrataenite and ordinary taenite with various relative ratios by the first heating procedure. It could be approximately assumed that the original tetrataenite domains contain 51–56 wt% Ni while the original ordinary taenite contains 25–30 wt% Ni. Assuming then that the two phases are homogenized with various relative ratios by the heating to result in the Ni-content spectrum in taenite observed after the heating, the original contents of tetrataenite and paramagnetic taenite on the initial pre-heating condition can be estimated to be 30.8 and 41.4 wt% respectively. These estimations are based on the observed magnetic intensity at room temperature of the first-run cooling thermomagnetic curve, *i.e.* 133 emu/g, in which 36 emu/g can be attributed to kamacite magnetization and remaining 97 emu/g to taenite magnetization. If the estimated value of original content of tetrataenite, 31 wt%, is accepted, the magnetization intensity at room temperature of the first-run heating thermomagnetic curve should be 49 emu/g (tetrataenite magnetization)+36 emu/g (kamacite magnetization)=85 emu/g, which is in approximate agreement with the observed value, shown in Fig. 16.

In the present magnetic analysis, the relative abundances of kamacite of 5 wt% Ni, tetrataenite and ordinary taenite of about 27 wt% Ni in the original unheated state are estimated to be 18.5, 34.8 and 46.7 in weight percent of the whole metallic component. The relative abundances of the three phases of metallic component, thus magnetically estimated, are considerably different from those obtained by a Mössbauer analysis (DANON *et al.*, 1979). However, the average Ni-content in the whole metallic component is 32.7 wt% in the magnetic analysis, while it is 32.6 wt% in the Mössbauer analysis. It could be reasonably presumed at the present stage that the differentiation into the three different phases is considerably different in different parts of St. Séverin chondrite, probably owing to local variety of metamorphism, though the chemical composition of the original melt metal is same.

4.4. Natural remanent magnetization

Changes in intensity and direction of NRM of St. Séverin by an AF-demagnetization up to 1000 Oe peak are shown in Fig. 18. As the experimental examination of NRM of St. Séverin was carried out before the discovery of tetrataenite and before an establishment of experimental facilities of AF-demagnetizing up to 1800 Oe peak, NRM characteristics of this chondrite for AF-demagnetization beyond 1000 Oe peak are not known yet. In Fig. 18, the NRM intensity can be demagnetized to about a half of the original intensity and the NRM direction is kept within about 30° in angle from the original direction during the course of AF-demagnetization up to 1000 Oe peak. Therefore, NRM of St. Séverin also is highly stable. It will be certain that a

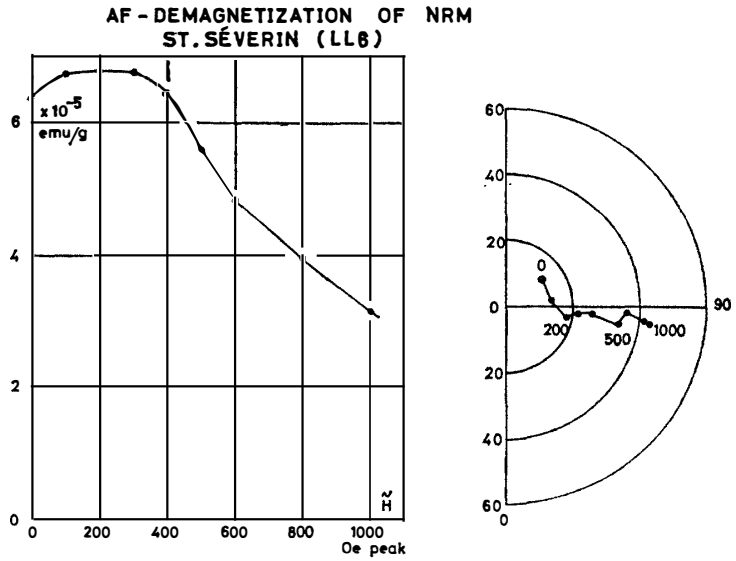

Fig. 18. AF-demagnetization curves of NRM of St. Séverin. Right: Direction. Numeral figures indicate $\tilde{H}$-values. Left: Intensity.

hard component of NRM, which cannot be AF-demagnetized by 1000 Oe peak, is possessed by tetrataenite grains, because ferromagnetic constituents in St. Séverin in its original state are only kamacite and tetrataenite.

Experimental tests of ARM-acquisition and AF-demagnetization of ARM were carried out for St. Séverin also in order to examine the soft component which can be identified to kamacite phase. The observed ARM acquisition curve approaches to saturation by $\tilde{H}=1000$ Oe peak, where ARM acquired by $\tilde{H}=300$ Oe peak occupies about 2/3 of the saturated value. A linear relationship between the AF-demagnetization curves of ARM and NRM holds for $\tilde{H}$-field range of 300–800 Oe peak, which gives $F_p=0.40/f_0$ Oe. The AF-demagnetization characteristics of the soft component of NRM of St. Séverin are, therefore, similar to those of ALH-77260 (A) and (C). Namely, these chondrites keep relatively small amounts of the soft component NRM in comparison with their capability of its acquisition.

5. Concluding Remarks—General Magnetic Properties of Tetrataenite-Rich Chondrites

The presence of tetrataenite grains has been confirmed in three chondrites, Yamato-74160 (LL7), ALH-77260 (L3) and St. Séverin (LL6). The chemical composition of tetrataenite-like metallic grains in Yamato-74160 and ALH-77260 measured by EPMA is represented by 45–52 wt% Ni and 48–55 wt% Fe in relative abundance of Fe and Ni, which are close to the composition of tetrataenite. Several comparatively large grains of the chemical composition are optically identified to tetrataenites because of their optical anisotropy, but it is not certain whether all metallic grains having the chemical composition are of tetrataenite structure or ordinary disordered taenite. On the other hand, the presence of tetrataenite phase in St. Séverin has been certainly confirmed by Mössbauer analysis (DANON *et al.*, 1979b).

In thermomagnetic analyses, a magnetic phase which appears to correspond to tetrataenite has its Curie point in a temperature range between 550°C to 580°C, which indicate that Ni-content in Fe-Ni alloy grains ranges between 56 and 61 wt% (*e.g.* CRANGLE and HALLAM, 1963). The magnetically estimated Ni-content is always a little larger than Ni-content in selected metallic grains directly measured by EPMA. As the metallic grains in chondrites comprise Fe, Ni and Co, it would be necessary to more precisely determine the thermomagnetic characteristics of Fe-Ni-Co alloys (less than 2 wt% in Co-content) as the basic data for meteorite magnetism.

On the basis of the present stage of knowledge, magnetic properties of tetrataenite-rich chondrites obtained from the present study may be summarized as follows:

(1) Magnetic coercive force

Magnetic coercive force (H_C) of the three chondrites examined in the present study is unusually large, in particular, in Yamato-74160 (H_C=255 Oe) and St. Séverin (H_C=500 Oe). The large value of H_C is due to presence of tetrataenite phase which has an extremely large value of H_C (about 5×10^3 Oe). As the magnetically hard tetrataenite phase coexists with other magnetically soft phases, the resultant bulk coercive force takes an intermediate value between the hard and soft components.

(2) Thermomagnetic curve characteristics

The thermomagnetic curves of the three tetrataenite-rich chondrites measured in an external magnetic field of 5–10 kOe are characterized by a very small decreasing rate of magnetization with increasing temperature up to 400–450°C and then a sharp decrease of magnetization to zero at Curie point when temperature approaches to Curie point. It has been reported (WASILEWSKI, 1982) that the same characteristics are observed also in other tetrataenite-rich meteorites such as Estherville (mesosiderite) and Bjurbole (L4).

A possible interpretation of the thermomagnetic curve characteristics will be an effect of the demagnetizing factor of tetrataenite grains whose magnetization along [110] and [111] axes are not saturated in magnetic fields smaller than 10 kOe (Appendix A.2). Another possible additional interpretation will be a gradual transformation of tetrataenite to ordinary taenite at temperatures above 320°C, which results in a decrease of magnetic anisotropy energy and consequently an increase of magnetization so that thermomagnetic curve becomes flat with increasing temperature until it sharply decreases near Curie point.

(3) Natural remanent magnetization

NRM of the three tetrataenite-rich chondrites contains a very hard component which connot be demagnetized by alternating magnetic fields larger than 1000 Oe peak. In Yamato-74160 and ALH-77260 chondrites, the hard component of NRM is kept almost constant for AF-demagnetization up to 1800 Oe peak. It will be certain that the hard component of NRM is possessed by tetrataenite phases in these chondrites, because the experimental result indicates that coercive force of the NRM hard component is larger than 1800 Oe. It is hoped then that coercivity and other magnetic characteristics of the hard tetrataenite remanent magnetization can be quantitatively determined in future studies.

(4) Effects of heat treatments

All the three tetrataenite-rich chondrites examined contain other ferromagnetic

metallic components. By heating up to elevated temperatures above 320°C in the ordinary vacuum circumstance of 10^{-5}–10^{-4} Torr atmosphere, it seems that tetrataenite is transformed to ordinary disordered taenite. It has been reported that the superlattice structure of tetrataenite is broken down at 450°C over a time scale of about 10 hours (DANON *et al.*, 1979a). It seems likely in the present experiments that tetrataenite is broken down to ordinary taenite during a time scale of less than several minutes at 800°C.

As discussed in individual cases of Yamato-74160, ALH-77260 and St. Séverin, it seems that a heating procedure of these chondrites up to about 800°C more or less causes a homogenization of different phases of different Ni-contents. In particular, it is clearly shown in Fig. 16 for St. Séverin that tetrataenite grains of 0.15–0.30 μm in grain size are homogenized with surrounding ordinary taenite matrix of about 27 wt% in Ni-content to newly form ordinary taenites of 30–52 wt% Ni by heating up to about 800°C. As suggested by this typical example, metallic components in the three chondrites examined in the present study are more or less altered by a heating procedure up to about 800°C to result in a homogenization with associated other components or a change in Ni-content. For example, kamacite component in ALH-77260, A, B and C, is considerably reduced in the second heating curve in comparison with the first heating curve, suggesting that a part of kamacite is homogenized with tetrataenite or ordinary taenite by the heating. Even a small amount of kamacite in the first heating curve of Yamato-74160 (Fig. 4) is much reduced in the second heating curve caused by the heating procedure. Curie point of tetrataenite phase is lowered by a heating procedure to that of the transformed ordinary taenite, suggesting that Ni-content in the original state is reduced during a process of transformation by the heating (see Appendix A.2). It seems highly necessary, therefore, that changes in composition and structure of these metallic components by heating are examined in fair detail.

(5) Unsolved problems

One of the most important problems regarding tetrataenites in chondrites will be how tetrataenite phase was formed in chondrites in the natural condition in the extraterrestrial space. Several investigators working on tetrataenite in meteorites (*e.g.* DANON *et al.*, 1979; METHA *et al.*, 1980; ALBERTSEN *et al.*, 1980; CLARKE and SCOTT, 1980) are inclined to presume that the ordered structures of tetrataenite may have formed when the meteorite parent body slowly cooled below the order-disorder transition temperature (320°C). It seems likely that this kind of presumption is most plausible.

The other important problem would be a possible acquisition mechanism of stable NRM possessed by the tetrataenite phase. In a simplest possible interpretation, an acquisition of the so-called thermo-chemical remanent magnetization (TCRM) may have taken place during the process of transformation from ordinary disordered taenite to tetrataenite in the course of slow cooling. As shown by a thermal demagnetization curve of the hard NRM component of Yamato-74160 in Fig. 6, however, the hard NRM possessed by tetrataenite phase in Yamato-74160 is practically constant up to about 230°C and thermally demagnetized by only a little portion in a heating process from 230 to 430°C and largely thermally demagnetized in the course of heating from 430 to 530°C. The TRM acquisition process indicates qualitatively the same characteristic as the thermal demagnetization curve of NRM, as shown in Fig. 7. If the TRM

acquisition process for tetrataenite is quantitatively parallel to that for the ordinary taenite of the same chemical composition, the majority of NRM may have been acquired during cooling process from 560 to 320°C as TRM by taenite grains which were still of ordinary taenite structure. The transformation from the ordinary taenite structure to the tetrataenite structure may have taken place at and below 320°C during the cooling process of the meteorite. Nothing has been known yet about what may happen about possible changes of TRM during the process of transformation from ordinary taenite to tetrataenite at and below 320°C. This problem will have to be carefully studied experimentally and theoretically in the future.

Acknowledgments

The writers' thanks are due to H. TAKEDA and K. YANAI for their suggestions on tetrataenite-rich chondrites from mineralogical viewpoints, and to N. SUGIURA for his assistance in laboratory experiments on St. Séverin chondrite in early time.

References

ALBERTSEN, J. F., JENSEN, G. B. and KNUDSEN, J. M. (1978): Structure of taenite in two iron meteorities. Nature, **273**, 453–454.

ALBERTSEN, J. F., JENSEN, G. B., KNUDSEN, J. M. and DANON, J. (1980): On superstructure in meteoritical taenite (abstract). Meteoritics, **13**, 379–383.

CLARKE, R. S., Jr. and SCOTT, E. R. D. (1980): Tetrataenite—ordered FeNi, a new mineral in meteorites. Am. Mineral., **65**, 624–630.

CRANGLE, J. and HALLAM, G. C. (1963): The magnetism of face-centered cubic and body-centered cubic iron-nickel alloys. Proc. R. Soc. London, **A272**, 119–132.

DANON, J., SCORZELLI, R., SOUZA AZEVEDO, I., CUROELLO, W., ALBERTSEN, J. F. and KNUDSEN, J. M. (1979a): Iron nickel 50–50 superstructure in the Santa Catharina meteorite. Nature, **277**, 283–284.

DANON, J., SCORZELLI, R. B., SOUZA AZEVEDO, I. and CHRISTOPHE MICHEL-LÉVY, M. (1979b): Iron-nickel superstructure in metal particles of chondrites. Nature, **281**, 469–451.

GOOLEY, R., MERRILL, R. B. and SMYTH, J. R. (1975): Anisotropic taenite in meteorites (abstract). Meteoritics, **10**, 410.

HALL, R. C. (1959): Single crystal anisotropy and magnetostriction constants of several ferromagnetic materials including alloys of NiFe, SiFe, AlFe, CoNi and CoFe. J. Appl. Phys., **30**, 816–819.

LOVERING, J. F. and PARRY, L. G. (1962): Thermomagnetic analysis of co-exsting nickel-iron metal phases in iron meteorites and the thermal histories of the meteorites. Geochim. Cosmochim. Acta, **26**, 361–382.

MASON, B. (1981): ALHA77260. Antarct. Meteorite Newsl., **4** (1), 49.

MEHTA, S., NOVOTNY, P. M., WILLIAMS, D. B. and GOLDSTEIN, J. I. (1980): Electron-optical observations of ordered FeNi in the Estherville meteorite. Nature, **284**, 151–153.

NAGATA, T. (1979): Meteorite magnetism and the early solar system magnetic field. Phys. Earth Planet. Inter., **20**, 324–341.

NAGATA, T., FISHER, R. M. and SCHWERER, F. C. (1972): Lunar rock magnetism. Moon, **4**, 160–186.

NAGATA, T., FISHER, R. M. and SCHWERER, F. C. (1974): Some characteristic magnetic properties of lunar materials. Moon, **9**, 63–77.

NÉEL, L., PAULEVE, J., PAUTHENET, R., LAUGIER, J. and DAUTREPPE, D. (1964): Magnetic properties of an iron-nickel single crystal ordered by neutron bombardment. J. Appl. Phys., **35**, 873–876.

SCOTT, E. R. D. and CLARKE, R. S., Jr. (1979): Identification of clear taenite in meteorites as ordered FeNi. Nature, **281**, 360–362.

TAKEDA, H. and YANAI, K. (1980): Strongly recrystallized meteorites from Antarctica; Yamato-74160 and ALHA-77081. Meteoritics, **15**, 373.

TAKEDA, H., DUKE, M. B., ISHII, T., HARAMURA, H. and YANAI, K. (1979): Some unique meteorites found in Antarctica and their relation to asteroids. Mem. Natl Inst. Polar Res., Spec. Issue, **15**, 54–76.

WASILEWSKI, P. J. (1982): Magnetic characterization of tetrataenite and its role in the magnetization of meteorite (abstract). Lunar and Planetary Science XIII. Houston, Lunar Planet. Inst., 843–844.

(Received August 19, 1982)

Appendix

A.1. Magnetic coercive force of a mixture of 2 ferromagnetics

A magnetization curve of a ferromagnetic phase of I_R in saturated IRM and H_C is coercive force can be approximated by a linear line in a range of magnetic field (H) of $-H_C \leq H \leq 0$, where $H_C > 0$. When a ferromagnetic specimen consists of two phases, *i.e.* (a) phase of $I_R^{(a)}$ and $H_C^{(a)}$ and (b) phase of $I_R^{(b)}$ and $H_C^{(b)}$, and relative abundances of (a) and (b) phases in unit of the mixed ferromagnetics are m and $(1-m)$ respectively, we get

$$I_R = mI_R^{(a)} + (1-m)I_R^{(b)} \tag{A-1}$$

and

$$mI^{(a)}(-H_C) + (1-m)I^{(b)}(-H_C) = 0,$$

where I_R is saturated IRM of the mixed ferromagnetics and $I^{(a)}(H)$ and $I^{(b)}(H)$ denote magnetization intensities of (a) and (b) phases respectively in magnetic field H. Then, coercive force, H_C, of the mixed ferromagnetics is given by

$$\frac{I_R}{H_C} = m\frac{I_R^{(a)}}{H_C^{(a)}} + (1-m)\frac{I_R^{(b)}}{H_C^{(b)}}. \tag{A-2}$$

In case of Yamato-74160, (a) and (b) phases are designated respectively to tetrataenite and ordinary taenite of the same chemical composition. As the tetrataenite phase can be assumed to be completely transformed after the heat treatment, $I_R^{(b)}$ and $H_C^{(b)}$ can be estimated from the observed parameters I_s, I_R and H_C of magnetic hysteresis curves of the bulk chondrite after the heating. I_R and H_C also can be estimated from the observed magnetic hysteresis curves of the bulk chondrite before the heating. In estimating $I_R^{(b)}$ and I_R, it is assumed that ratio I_R/I_s is same in the metallic component and in the bulk chondrite and $I_s = 160$ emu/g (*e.g.* CRANGLE and HALLAM, 1963). On the other hand, $H_C^{(a)}$ of tetrataenite can be roughly evaluated as $H_C^{(a)} = 2K_1/J_s = 4.9 \times 10^3$ Oe, where $J_s = 1.3 \times 10^3$ emu/cm^3. Thus, $I_R = 15.37$ emu/g, $H_C = 255$ Oe, $I_R^{(b)} = 0.52$ emu/g, $H_C^{(b)} = 8$ Oe and $H_C^{(a)} = 4900$ Oe are known from experimental results. Then, two unknown values, m and $I_R^{(a)}$, are evaluated by eqs. (A-1) and (A-2) as

$$m = 0.40, \qquad I_R^{(a)} = 24.9 \text{ emu/g}.$$

In case of ALH-77260, at least three ferromagnetic phases, kamacite, tetrataenite and ordinary taenite, coexist in the original unheated state. Hence, the present method of analysis cannot be applied on ALH-77260.

In case of St. Séverin, two major ferromagnetic phases in the original unheated state at room temperature are (a) tetrataenite and (b) kamacite. Among magnetic parameters involved in eqs. (A-1) and (A-2), only I_R and H_C can be evaluated from experimental results and $H_C^{(a)}$ can be assumed to be 4.9×10^3 Oe. However, a magnetic analysis of St. Séverin suggests that $m=0.65$, because ratio of abundance of tetrataenite to kamacite is estimated as 30.8: 16.4 wt%. If we assume further that $I_R^{(a)}$ for tetrataenite is same as evaluated for Yamato-74160 tetrataenite phase, namely $I_R^{(a)}=24.9$ emu/g, we can get

$$I_R^{(b)}=12.3 \text{ emu/g}, \qquad H_C^{(b)}=115 \text{ Oe},$$

for the kamacite phase. This result may suggest that the kamacite phase in St. Séverin is mostly in form of fine single magnetic domain having a considerably large shape anisotropy to result in $H_C^{(b)}=115$ Oe.

A.2. Thermomagnetic curve of tetrataenite

One of possible reasons for the observed flat thermomagnetic curve of tetrataenite in a temperature range from room temperature to 400–450°C and its sharp decrease toward Curie point, and for the observed relative reduction of magnetization intensity of tetrataenite in comparison with that of ordinary taenite of the same chemical composition in a magnetic field of 5–10 kOe, would be an effect of the demagnetizing factor of metallic grains, because the magnetization curve of tetrataenite is subjected to a large magnetic anisotropy (NÉEL *et al.*, 1964) as illustrated in Fig. A-1, where the magnetizations (J) of a tetrataenite single crystal along [100] and [110] axes *vs.* the effective magnetic field (H_{eff}) at room temperature are shown. In Fig. A-1, a straight line on the left diagram presents $H_{\text{eff}}=5000$ Oe$-NJ$, where N denotes the average de-

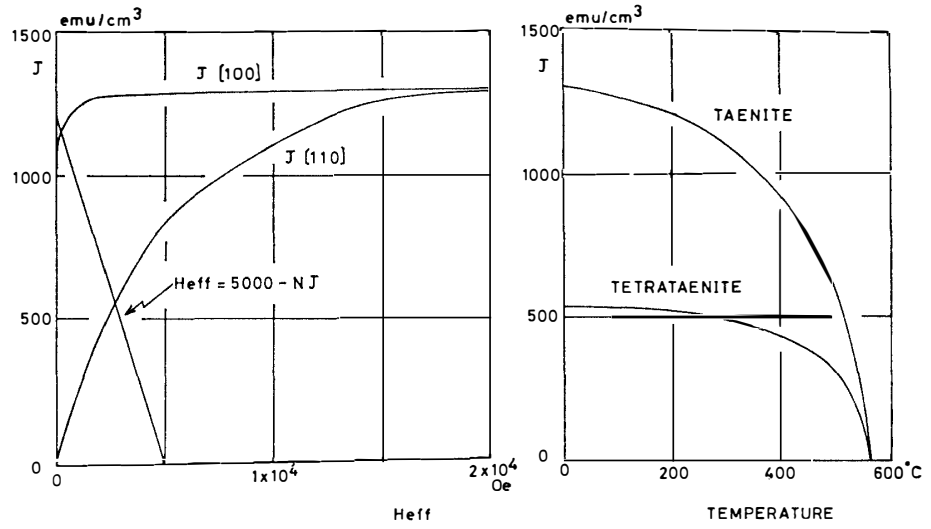

Fig. A-1. Model for reduction and modification of thermomagnetic curve of tetrataenite due to effects of demagnetizing factor of tetrataenite grains.
Left: Magnetization curves along [100] and [110] axes of tetrataenite crystal and a line of $H_{\text{eff}}=5$ kOe$-NJ$.
Right: Model thermomagnetic curves of ordinary taenite and tetrataenite in $H_{\text{ex}}=5$ kOe.

magnetizing factor of tetrataenite grains. When an external magnetic field $H_{ex}=5000$ Oe is applied, the corresponding magnetization is given by a cross point of $H_{eff}=5000 - NJ$ line and $J=J(H_{eff})$ curve.

It will be obvious that the magnetization along [110] axis of taenite in $H_{ex}=5000$ Oe is much smaller than that along [100] axis which is approximately equal to the magnetization of ordinary taenite in the same magnetic field. The right diagram of Fig. A-1 shows an example of a thermomagnetic curve of tetrataenite along [110] axis in $H_{ex}=$ 5 kOe derived on the basis of the above-mentioned assumption from a thermomagnetic curve of ordinary taenite, where N is reasonably assumed to be 4.0. The thermomagnetic curve for tetrataenite [110] axis becomes considerably flatter and smaller than that for ordinary taenite owing to the effect of demagnetizing factor of metallic grains.

It must be pointed out, however, that the thermomagnetic curve of tetrataenite [110] axis never crosses that of ordinary taenite, whereas the first heating thermomagnetic curves of Yamato-74160, ALH-77260 and St. Séverin are always crossed by their first cooling and second heating and cooling thermomagnetic curves. This observed fact may suggest a possibility that Curie point of the ordinary taenite transformed from tetrataenite by the heating is spread over a certain lower temperature range by a reduction of Ni-content in the transformed ordinary taenite phase by homogenizing the Ni-rich tetrataenite phase with Ni-poorer taenite phase or kamacite phase. In the observed thermomagnetic curves, Curie point at 560°C in the first heating curve is lowered to 540°C in the first cooling curve for Yamato-74160 (Fig. 4), Curie point at 585°C in the first heating curve (Fig. 11a) to 560°C in the second heating curve (Fig. 12a) for ALH-77260 B, Curie point at 570°C in the first heating curve (Fig. 11b) to 565°C in the second heating curve (Fig. 12b) for ALH-77260 C, and Curie point at 585–565°C for ALH-77260 A (Fig. 13). It is already discussed in some detail in Section 4 that Curie point of homogenized taenite after the heating procedure is spread over a wide temperature range below 550°C which is Curie point of the original tetrataenite for St. Séverin. Such possible metallographical changes presumed from magnetic data will have to be examined by direct metallographical observations in the future.

It must be further pointed out that the flatness of thermomagnetic curve of tetrataenite expected from the model of effects of demagnetizing factor of metallic grains seems to be still insufficient in comparison with the observed data shown in Figs. 4, 11, 13 and 16. Another possible cause, and probably an additional possible cause, of the observed flatness of thermomagnetic curve of tetrataenite would be an effect of a slowly increasing transformation of tetrataenite to ordinary taenite with increasing temperatures above the order-disordered transformation temperature of tetrataenite (320°C). As already discussed, the magnetization intensity of ordinary taenite phase in $H_{ex}=$ 5–10 kOe is larger than that of tetrataenite phase even if tetrataenite crystalls are oriented at random. Hence, a transformation from tetrataenite to ordinary taenite should result in an increase of magnetization in H_{ex}, and a time rate of the transformation should increase with increasing temperature. If a decrease of spontaneous magnetization intensity (J) of tetrataenite with increasing temperature with a constant speed (200 degrees/hour) could be almost compensated by a continuously increasing magnetization caused by the transformation from tetrataenite to ordinary taenite, the observed thermomagnetic curve will become nearly flat. Since Curie point of tetratae-

nite is the same as that of ordinary taenite of the same chemical composition, a decrease of magnetization of tetrataenite under the above-mentioned condition of slow partial transformation to ordinary taenite should be very sharp when temperature approaches Curie point. Both effects of the demagnetizing factor of tetrataenite grains and the transformation from tetrataenite to ordinary taenite above 320°C are theoretically possible for interpreting the observed flatness of thermomagnetic curve up to 400–450°C and its sharp decrease near Curie point. These possible effects will have to be experimentally checked in future studies.